A ROBUST AND EFFICIENT SENSITIVITY ANALYSIS METHOD FOR AEROELASTIC DESIGN OPTIMIZATION

Manuel Barcelos, ManuelBarcelos@unb.br
Kurt Maute, maute@colorado.edu
Institution and address for first and second authors - if the same

Abstract. *In recent years, the development of faster computers and parallel processing allowed the application of high-fidelity analysis methods for aeroelastic design optimization of aircraft. For practical reasons most of the research in aeroelastic optimization, treat the aeroelastic system as a quasi-static problem. This work is concerned with the creation of a robust and efficient aeroelastic optimization methodology for viscous laminar and turbulent flows by using high-fidelity sensitivity analysis techniques. For quasi-static aeroelastic problems, the traditional staggered sensitivity analysis solution strategy has unsatisfactory performance when applied to cases where there is a strong fluid-structure coupling. Consequently, this work also proposes a solution methodology for aeroelastic sensitivity analyses of quasi-static problems, which is based on the fixed point of an iterative nonlinear block Gauss-Seidel scheme. The methodology can also be interpreted as the solution of the Schur complement of the aeroelastic sensitivity analysis linearized systems of equations. The methodologies developed in this work are tested and verified by using realistic aeroelastic systems.*

Keywords: *Sensitivity Analysis, Aeroelasticity, Viscous Flow, Schur Complement, High-fidelity Analysis*

1. INTRODUCTION

In the past, aeroelastic design optimization was based on simplistic systems, combining linear structure and fluid models (Barthelemy et al., 1994) such as beam elements and panel methods. Advances in computational resources led to the creation of sophisticated finite element and finite volume methods, capable of accounting for nonlinear structure and fluid theories. These advanced techniques were soon assimilated into structural and aerodynamic design optimization (Turgeon, Pelletier and Borggaard, 2004). For the structure, finite element methods allowed the modeling of material and geometric nonlinearities (Pajot and Maute, 2006). For the fluid field, the finite volume discretization of the Euler and Navier-Stokes equations allowed the capture of nonlinear aerodynamic behaviors such as shock waves, flow separation and vorticity propagation, respectively (Guezaine, 1999). The occurrence of turbulence models added turbulent effects to conventional finite volume discretizations (Cebeci, T., 2004). For some time, the difficulty in coupling advanced computational methods to simulate aeroelastic systems was the deformation of the fluid mesh, especially for complex geometries. This difficulty was efficiently solved with the incorporation of pseudo-elastic mesh motion schemes to the problem as an additional field (Degand. and Farhat, 2002).

Only recently, with the popularization of faster and less expansive parallel processing machines, advanced computational methods found their way into aeroelastic design optimization (Nikbay, 2002). However, the majority of the optimization methodologies still use inviscid schemes based on the Euler equations discretization to overcome difficulties referent to computational cost. Due to the increasing need for fidelity, some optimization methodologies already start to consider viscous turbulent effects on small scale aeroelastic problems (Lund, Møller and Jakobsen, 2003) by using eddy viscosity turbulence models coupled with averaged discretizations of the Navier-Stokes equations. For simplicity, these methodologies are based on a monolithic representation of the structure and fluid domains. Consequently, these approaches lack robustness and efficiency to tackle large-scale realistic aeroelastic systems. The optimization methodology presented here integrates up-to-date CFD and CSM analysis tools developed at the Center for Aerospace Structures (CAS) at the University of Colorado (Farhat, Geuzaine and Brown, 2003) to the optimization framework created by Maute, Nikbay and Farhat (2001a).

So far, large scale quasi-static aeroelastic design optimization problems relied essentially on staggered (or segregated) solvers based on block Gauss-Seidel schemes to solve the FSI sensitivity analysis problem. The staggered solvers are proven accurate and efficient for most of the loosely-coupled quasi-static FSI problem configurations. However, there are certain configurations that staggered solvers lack robustness and efficiency (Barcelos, Bavestrello and Maute, 2004), specially when the coupling between fluid and structure is strong which increases even more the global sensitivity equations (GSE) natural ill conditioning state leading to convergence issues (Barcelos, Bavestrello and Maute, 2006). The goal of this work is to solve the shortcomings of Gauss-Seidel schemes by increasing the robustness and efficiency of quasi-static aeroelastic sensitivity analysis in the context of design optimization. The methodology proposed is based on the solution of the Schur complement on the derivatives of the degrees of freedom of the fluid-structure interface of the GSE. A Krylov method is suggested as solver for the linear condensed system of equations. This methodology is derived from a fixed point strategy applied to the fluid-structure interface derivative of the degrees of freedom, and only requires few modifications to existing computational tools. The methodology is referred to as Schur-Krylov (SK) method because the GSE are linear. In this work, the SK method is tested in the design optimization of realistic problems, and compared to traditional

staggered solvers. The remainder of this paper is organized as follows: in section 2, the aeroelastic optimization is introduced. Sections 3 presents the three-field formulation of the aeroelastic and sensitivity analysis problems. In section 4, the conventional block Gauss-Seidel approach presented, and the alternative SK method for solving the aeroelastic sensitivity analysis is outlined. In section 5 the robustness and efficiency of the solution approaches for aeroelastic sensitivity analysis is studied by numerical examples based on realistic wings. Finally, the section 6 summarizes the outcomes of the numerical studies.

2. Aeroelastic Optimization

An optimization problem can be expressed as the minimization of an objective function under certain equality and inequality constraints (Maute, Nikbay and Farhat, 2001a). The formulation of a generic optimization problem is defined as:

$$\min_{\boldsymbol{s}\in\mathbb{S}} z(\boldsymbol{q}(\boldsymbol{s}),\boldsymbol{s}) \tag{1}$$

$$h(\boldsymbol{q}(\boldsymbol{s}),\boldsymbol{s}) = 0 \qquad h \in \mathbb{R}^{n_h} \tag{2}$$

$$g(\boldsymbol{q}(\boldsymbol{s}),\boldsymbol{s}) \geq 0 \qquad g \in \mathbb{R}^{n_g} \tag{3}$$

$$\mathbb{S} = \{\boldsymbol{s} \in \mathbb{R}^{n_s} | s_i^L \leq s_i \leq s_i^U\} \tag{4}$$

where $\boldsymbol{q}$ is the set of design criteria and which component s_i of the set of design variables ($\boldsymbol{s}$) is limited by lower (s_i^L) and upper (s_i^U) bounds. In an aeroelastic design optimization framework, the abstract design variables are defined by structural and aerodynamic parameters, such as geometry or shape, dimensions of the structural components, free stream Mach number and angles of attack of the flow. The design criteria are associated with quantities which describe aerodynamic performance and structural behavior, such as aerodynamic forces and moments, structural displacement, stress and mass. For an aeroelastic optimization problem, the design criteria are dependent on the response of the aeroelastic system, which is characterized by the vector of structural displacements ($\boldsymbol{u}$) and the vector of fluid state variables ($\boldsymbol{w}$). The aeroelastic response is also a function of the design variables.

3. Aeroelastic and Sensitivity Analyses Formulation

This section presents the aeroelastic analysis and the sensitivity analysis procedures from a numerical point of view. The formulation of the aeroelastic problem and the sensitivity computation are discussed in detail. The aeroelastic problem is defined by a three field formulation which establishes integration among structure, fluid mesh motion and fluid subproblems.

3.1 Aeroelastic Analysis

In a general optimization framework, for a given design variable $\boldsymbol{s}$, the design criteria are computed by solving the discrete aeroelastic equations for the aeroelastic response. The governing equations in semi-discrete form are written as:

$$\mathcal{S}(\boldsymbol{u},\dot{\boldsymbol{u}},\ddot{\boldsymbol{u}},\boldsymbol{x},\dot{\boldsymbol{x}},\boldsymbol{w};\boldsymbol{s}) \tag{5}$$

$$\mathcal{M}(\boldsymbol{u},\dot{\boldsymbol{u}},\boldsymbol{x},\dot{\boldsymbol{x}},\ddot{\boldsymbol{x}};\boldsymbol{s}) \tag{6}$$

$$\mathcal{F}(\boldsymbol{x},\dot{\boldsymbol{x}},\boldsymbol{w},\dot{\boldsymbol{w}};\boldsymbol{s}) \tag{7}$$

where $\mathcal{S}$ is the state equation of the structure, $\mathcal{M}$ is the equation which governs the motion of the fluid mesh and $\mathcal{F}$ is the state equation of the fluid. The discrete vectors $\boldsymbol{u}$, $\boldsymbol{x}$ and $\boldsymbol{w}$ represent the structural displacements, the motion of the fluid mesh and the fluid state variables respectively. The dot sign represents the total derivative with respect to time. During an aeroelastic analysis procedure, the design variables are constant and consequently omitted in the formulation and the discretization of the aeroelastic equations. Most of the aircraft design requirements, such as lift and drag at take-off, cruise and landing are effectively computed by using stead state flow configurations. Therefore, an aeroelastic optimization procedure based on a quasi-static methodology is enough to represent with high-fidelity the whole problem. The terms related to the time derivative are neglected.

3.1.1 Structure Subproblem

The discrete state equation of the structure is built as:

$$\mathcal{S}(\boldsymbol{u},\boldsymbol{x},\boldsymbol{w}) \equiv \boldsymbol{f}_{int}(\boldsymbol{u}) - \boldsymbol{f}_{ext}(\boldsymbol{x},\boldsymbol{w}) = \boldsymbol{0} \tag{8}$$

$\boldsymbol{f}_{int}$ and $\boldsymbol{f}_{ext}$ are the internal and external forces acting on the structure. If the structural model accounts for geometric and/or material nonlinearities, the internal forces are nonlinear functions of the displacements $\boldsymbol{u}$. However, if the structure

is linear, the internal forces are simplified to:

$$\boldsymbol{f}_{int}(\boldsymbol{u}, \dot{\boldsymbol{u}}) = \mathbf{K}\boldsymbol{u} \tag{9}$$

$$\boldsymbol{f}_{ext}(\boldsymbol{x}, \boldsymbol{w}) = \boldsymbol{f}_0 + \boldsymbol{f}_{ae}(\boldsymbol{x}, \boldsymbol{w}) \tag{10}$$

where $\mathbf{K}$ denote the linear stiffness matrix of the structure, and the spatial discretization of the structural equations is obtained through finite element. The external forces (equation 10) are written as a combination of aerodynamic loads ($\boldsymbol{f}_{ae}$) and structural loads due to gravity and variation of temperature, among other, here denoted by $\boldsymbol{f}_0$. The aerodynamic loads $\boldsymbol{f}_{ae}$ represent the action of the fluid force $\boldsymbol{f}_\Gamma$ on the structure mesh through the interface $\Gamma_{F/S}$. The fluid force is transferred to the structure domain by using a transformation matrix ($\mathbf{T}_f$), which is built based on the conservation of energy and momentum through the boundary between fluid and structure (Farhat, Lesoinne and LeTallec, 1998).

$$\boldsymbol{f}_{ae}(\boldsymbol{x}, \boldsymbol{w}) = \mathbf{T}_f \boldsymbol{f}_\Gamma(\boldsymbol{x}, \boldsymbol{w}) \tag{11}$$

3.1.2 Fluid Mesh Subproblem

The governing equation of the motion of the fluid mesh (equation 6) is built considering the fluid mesh as a pseudo-elastic structure (Batina, 1991, Farhat, Lesoinne and LeTallec, 1998, Degand and Farhat, 2002):

$$\mathcal{M}(\boldsymbol{u}, \boldsymbol{x}(\mathbf{x})) \equiv \bar{\mathbf{K}}\mathbf{x} = \bar{\mathbf{R}} \quad \therefore \quad \begin{pmatrix} \bar{\mathbf{K}}_{\Omega\Omega} & \bar{\mathbf{K}}_{\Omega\Gamma} \\ \bar{\mathbf{K}}_{\Omega\Gamma} & \bar{\mathbf{K}}_{\Gamma\Gamma} \end{pmatrix} \begin{pmatrix} \mathbf{x}_\Omega \\ \mathbf{x}_\Gamma \end{pmatrix} = \begin{pmatrix} \bar{\mathbf{R}}_\Omega \\ \bar{\mathbf{R}}_\Gamma \end{pmatrix} \tag{12}$$

The fictitious stiffness matrix $\bar{\mathbf{K}}$ and the reaction force vector $\bar{\mathbf{R}}$ in equation 12 can be divided in subsets related to the internal (Ω) and external (Γ) degrees of freedom of the fluid mesh. The quasi-static fluid mesh motion equations obey the kinematic compatibility between fluid and structure. The kinematic compatibility dictates how the position $\mathbf{x}_\Gamma$ of fluid mesh on the boundary $\Gamma_{F/S}$ is related to the structural displacement by the transformation:

$$\mathbf{x}_\Gamma = \mathbf{T}_u \boldsymbol{u} \tag{13}$$

The operator $\mathbf{T}_u$ is a transformation matrix that converts the structural displacement into motion of the fluid mesh on $\Gamma_{F/S}$. For conservative fluid-structure coupling $\mathbf{T}_f = \mathbf{T}_u^T$. Equation 12 is solved with the condition of null force on the internal grid points ($\bar{\mathbf{R}}_\Omega = \mathbf{0}$) by using a finite element method. The fictitious matrix ($\bar{\mathbf{K}}$) is constructed by an improved spring analogy method (Degand and Farhat, 2002).

3.1.3 Fluid Subproblem

The discrete state equation of the fluid (equation 7) is the result of a finite element or a finite volume spatial approximation of the arbitrary Lagrangian-Eulerian (ALE) conservative form of the Navier-Stokes equations and Spalart-Allmaras turbulence model. $\mathbf{F}$ is the numerical flux vector resulting from the approximation of the integral of the physical flux function over the cells of the fluid mesh.

$$\mathcal{F}(\boldsymbol{x}, \boldsymbol{w}) \equiv \mathbf{F}(\boldsymbol{x}, \boldsymbol{w}) = \mathbf{0} \tag{14}$$

3.2 Sensitivity Analysis

The crucial element of a gradient-base optimization methodology is an accurate and efficient design sensitivity analysis. The sensitivity analysis of nonlinear large-scale aeroelastic system represents a great computational effort. The main goal in a sensitivity analysis procedure is the computation of the derivative of the design criteria (q_j) with respect to the design variables ($\boldsymbol{s}_l$).

$$\frac{dq_j}{d\boldsymbol{s}_l} = \frac{\partial q_j}{\partial \boldsymbol{s}_l} + \left(\frac{\partial q_j}{\partial \boldsymbol{u}}\right)^T \frac{d\boldsymbol{u}}{d\boldsymbol{s}_l} + \left(\frac{\partial q_j}{\partial \boldsymbol{x}}\right)^T \frac{d\boldsymbol{x}}{d\boldsymbol{s}_l} + \left(\frac{\partial q_j}{\partial \boldsymbol{w}}\right)^T \frac{d\boldsymbol{w}}{d\boldsymbol{s}_l} \tag{15}$$

The partial derivatives $\partial q_j/\partial \boldsymbol{s}_l$, $\partial q_j/\partial \boldsymbol{u}$, $\partial q_j/\partial \boldsymbol{x}$ and $\partial q_j/\partial \boldsymbol{w}$ are directly calculated within the discretized models of the structure and of the fluid by using the relation of the structural and aerodynamic parameters with respect to the abstract optimization variables defined in the design model. The derivatives of the aeroelastic response $d\boldsymbol{u}/d\boldsymbol{s}_l$, $d\boldsymbol{x}/d\boldsymbol{s}_l$ and $d\boldsymbol{w}/d\boldsymbol{s}_l$ are obtained by solving the linear system of equations 16, also referred to as global sensitivity equations (GSE), resulting from the differentiation of the governing aeroelastic equations in discrete form 5-7 with respect to the

abstract optimization variables (Sobieszczanski-Sobieski, 1990).

$$\underbrace{\begin{pmatrix} \frac{\partial \mathcal{S}}{\partial \boldsymbol{u}} & \frac{\partial \mathcal{S}}{\partial \boldsymbol{x}} & \frac{\partial \mathcal{S}}{\partial \boldsymbol{w}} \\ \frac{\partial \mathcal{M}}{\partial \boldsymbol{u}} & \frac{\partial \mathcal{M}}{\partial \boldsymbol{x}} & \mathbf{0} \\ \mathbf{0} & \frac{\partial \mathcal{F}}{\partial \boldsymbol{x}} & \frac{\partial \mathcal{F}}{\partial \boldsymbol{w}} \end{pmatrix}}_{\mathbf{A}} \begin{pmatrix} \frac{d\boldsymbol{u}}{d\boldsymbol{s}_l} \\ \frac{d\boldsymbol{x}}{d\boldsymbol{s}_l} \\ \frac{d\boldsymbol{w}}{d\boldsymbol{s}_l} \end{pmatrix} = - \begin{pmatrix} \frac{\partial \mathcal{S}}{\partial \boldsymbol{s}_l} \\ \frac{\partial \mathcal{M}}{\partial \boldsymbol{s}_l} \\ \frac{\partial \mathcal{F}}{\partial \boldsymbol{s}_l} \end{pmatrix} \tag{16}$$

The partial derivative of the residuals $\partial\mathcal{S}/\partial\boldsymbol{s}_l$, $\partial\mathcal{M}/\partial\boldsymbol{s}_l$ and $\partial\mathcal{F}/\partial\boldsymbol{s}_l$ are directly calculated within the discretized models of the structure and the fluid, and the Jacobian matrix $\mathbf{A}$ is evaluated at the aeroelastic steady state. There are two basic methodologies to calculate the gradient of the design criteria when substituting the solution of the GSE (equation 16) into equation 15, the direct and the adjoint approaches. If the number of abstract optimization variable is smaller than the number of criteria, the most efficient methodology is the direct approach.

The entire sensitivity analysis procedure presented in this work employs analytical derivatives of the aeroelastic analysis algorithm which were developed manually. The manual differentiation is justified by using a CFD tool (Farhat, Geuzaine and Brown, 2003) which is organized in an object oriented class structure. The application of automatic differentiation is not always possible. Also, a manual differentiation allows a customized control of features, such as memory allocation and storage.

4. Aeroelastic and Sensitivity Analyses Solvers

The great majority of the methods employed to solve the coupled system of nonlinear equations (equations 5-7) are based on the nonlinear block Gauss-Seidel (NLBGS) scheme (Vrahatis, Magoulas and Plagianakos, 2003). The steps of this scheme are the main building blocks of staggered methods (Farhat and Lesoinne, 2000) for solving quasi-static and transient fluid-structure interaction (FSI) analysis. This configuration allows the application of a specific solver for each respective subproblem: structure, mesh motion and fluid.

In this work, the sensitivity analysis is based on the assumption that the aeroelastic system of equations is satisfied at the steady state solution. As a first attempt to solve the sensitivity analysis problem, the direct solution approach is developed for the sensitivity analysis of inviscid, viscous and turbulent aeroelastic systems. The entire sensitivity analysis procedure presented employs analytical derivatives of the aeroelastic analysis algorithm which were developed manually to allow a customized control of features, such as memory allocation and storage.

4.1 Direct sensitivity analysis method

The implementation of the direct solution approach primarily requires the solution of the GSE (equation 16), which is the linear system of equations resulting from the derivation of the discrete steady state aeroelastic equations (equations 8, **??** and 14) with respect to the abstract optimization variable (s_l).

$$\begin{pmatrix} \bar{\mathbf{K}}_{\Omega\Omega} & \mathbf{0} & \mathbf{0} & \bar{\mathbf{K}}_{\Omega\Gamma} \\ \frac{\partial \mathbf{F}}{\partial \mathbf{x}_\Omega} & \mathbf{H} & \mathbf{0} & \frac{\partial \mathbf{F}}{\partial \mathbf{x}_\Gamma} \\ -\mathbf{T}_f \frac{\partial \boldsymbol{f}_\Gamma}{\partial \mathbf{x}_\Omega} & -\mathbf{T}_f \frac{\partial \boldsymbol{f}_\Gamma}{\partial \boldsymbol{w}} & \mathbf{K} & -\mathbf{T}_f \frac{\partial \boldsymbol{f}_\Gamma}{\partial \mathbf{x}_\Gamma} \\ \mathbf{0} & \mathbf{0} & -\mathbf{T}_u & \mathbf{I} \end{pmatrix} \begin{pmatrix} \frac{d\mathbf{x}_\Omega}{ds_l} \\ \frac{d\boldsymbol{w}}{ds_l} \\ \frac{d\boldsymbol{u}}{ds_l} \\ \frac{d\mathbf{x}_\Gamma}{ds_l} \end{pmatrix} = - \begin{pmatrix} \mathbf{0} \\ \frac{\partial \mathbf{F}}{\partial s_l} \\ \frac{\partial \boldsymbol{f}_{int}}{\partial s_l} - \frac{\partial \boldsymbol{f}_{ext}}{\partial s_l} \\ \frac{\partial \mathbf{x}_\Gamma}{\partial s_l} \end{pmatrix} \tag{17}$$

where the explicit dependence of the fluid mesh on the shape variations is taken into account by introducing the term $\frac{\partial \mathbf{x}_\Gamma}{\partial s_l}$ (Maute, Nikbay and Farhat, 2001a). Once the derivative of the aeroelastic state variables is computed, the derivative of the optimization criterion with respect to the abstract optimization variable is determined by directly substituting it into the criterion expression (equation 15).

$$\frac{dq_j}{ds_l} = \frac{\partial q_j}{\partial s_l} - \begin{pmatrix} \frac{\partial q_j}{\partial \mathbf{x}_\Omega} \\ \frac{\partial q_j}{\partial \boldsymbol{w}} \\ \frac{\partial q_j}{\partial \boldsymbol{u}} \\ \frac{\partial q_j}{\partial \mathbf{x}_\Gamma} \end{pmatrix}^T \begin{pmatrix} \frac{d\mathbf{x}_\Omega}{ds_l} \\ \frac{d\boldsymbol{w}}{ds_l} \\ \frac{d\boldsymbol{u}}{ds_l} \\ \frac{d\mathbf{x}_\Gamma}{ds_l} \end{pmatrix} \tag{18}$$

The solution of the GSE in the direct sensitivity analysis approach is usually obtained by employing staggered solvers. Thus, the direct method in this text is introduced by using a staggered algorithm representation. However, previous works (Maute, Nikbay and Farhat, 2001a and 2001b) have shown that conventional staggered solvers demand more computational time in the sensitivity analysis than in aeroelastic analysis. Therefore, an alternative with great potential to accelerate the sensitivity analysis is to deduce the GSE by using the Schur complement formulation and to solve the reduced system with a Krylov method. This alternative algorithm is also explored in this work.

4.2 Linear block Gauss-Seidel scheme

The staggered solvers used in the sensitivity analysis of aeroelastic systems are based on a LBGS scheme. This staggered algorithm has similar steps to the NLBGS scheme. The main difference is that the LBGS scheme is applied to the GSE, which is a linear system, and the NLBGS is applied to the nonlinear aeroelastic system of equations. However, the disadvantage of the LBGS scheme is that the Jacobian matrix of the GSE is highly ill-conditioned when evaluated at the aeroelastic steady state ($\boldsymbol{u}^{(n)}$,$\boldsymbol{x}^{(n)}$,$\boldsymbol{w}^{(n)}$), specially for aeroelastic systems with strong coupling between fluid and structure.

The LBGS scheme is an iterative solver, and is subdivided in three main steps related to the solution: mesh motion, fluid and structure subproblems to obtain the derivative of the aeroelastic response (equation 16). After setting up the initial guess $\left(d\boldsymbol{u}^{(0)}/ds_l, d\boldsymbol{x}^{(0)}/ds_l, d\boldsymbol{w}^{(0)}/ds_l\right)$, the algorithm starts the iterative loop by solving the mesh motion subproblem. This first step consists in computing the derivative of the interior degrees of freedom with respect to the abstract optimization variables $\left(d\mathbf{x}_\Omega{}^{(m+1)}/ds_l\right)$ given the derivative of the degrees of freedom $\left(d\mathbf{x}_\Gamma{}^{(m)}/ds_l\right)$ on the fluid-structure boundary ($\Gamma_{F/S}$). The computation of $d\mathbf{x}_\Omega{}^{(m+1)}/ds_l$ is done by setting $d\mathbf{x}_\Gamma{}^{(m+1)}/ds_l = d\mathbf{x}_\Gamma{}^{(m)}/ds_l$ and solving an pseudoelastic problem similar to the one solved on the aeroelastic analysis,

$$\bar{\mathbf{K}}_{\Omega\Omega}(\boldsymbol{x}^{(0)})\frac{d\mathbf{x}_\Omega}{ds_l}^{(m+1)} = -\bar{\mathbf{K}}_{\Omega\Gamma}(\boldsymbol{x}^{(0)})\frac{d\mathbf{x}_\Gamma}{ds_l}^{(m+1)} \tag{19}$$

$$\frac{d\boldsymbol{x}}{ds_l}^{(m+1)} = \begin{pmatrix} \frac{d\mathbf{x}_\Omega}{ds_l}^{(m+1)} \\ \\ \frac{d\mathbf{x}_\Gamma}{ds_l}^{(m+1)} \end{pmatrix} \tag{20}$$

In the second step, the fluid subproblem is solved for the computation of the derivative of the fluid state variables $d\boldsymbol{w}/ds_l$. The linear system of equations obtained with the derivative of the fluid discretized equations is

$$\mathbf{H}(\boldsymbol{w}^{(n)})\frac{d\boldsymbol{w}}{ds_l}^{(m+1)} = -\frac{\partial\mathbf{F}}{\partial s_l} - \frac{\partial\mathbf{F}}{\partial\boldsymbol{x}}\frac{d\boldsymbol{x}}{ds_l}^{(m+1)} \tag{21}$$

Equation 21 has practically the same structure of the one defined for the NLBGS schemes, the matrix operators are identical. This represents an advantage because the same type of solver for linear system of equations can be applied in the aeroelastic analysis and the sensitivity analysis. In order to obtain consistent sensitivities, the finite volume and finite element discretization accuracy employed in the construction of the Jacobian matrix $\mathbf{H}$ and the flux $\mathbf{F}$ has to be identical to the one chosen for the aeroelastic analysis (Maute, Nikbay and Farhat, 2001a). After obtaining the derivative of the fluid state variables, the derivative of the fluid forces on the fluid-structure interface ($\Gamma_{F/S}$) are computed and transferred to the structural domain:

$$\frac{d\boldsymbol{f}_\Gamma}{ds_l}^{(m+1)} \rightarrow \frac{d\boldsymbol{f}_{ae}}{ds_l}^{(m+1)} = \mathbf{T}_f\left(\frac{\partial\boldsymbol{f}_\Gamma}{\partial\boldsymbol{x}}\frac{d\boldsymbol{x}}{ds_l}^{(m+1)} + \frac{\partial\boldsymbol{f}_\Gamma}{\partial\boldsymbol{w}}\frac{d\boldsymbol{w}}{ds_l}^{(m+1)}\right) \tag{22}$$

Quantities on the right-hand side of the fluid sensitivity equations (equation 21) and the derivative of fluid forces (equation 22) can also be evaluated by using finite differences, resulting in a methodology denominated as semi-analytical sensitivity analysis. The central finite differences are employed to increase accuracy. However, the analytical differentiation is preferred because of its efficiency and precision over the finite difference approach. The third step of the LBGS algorithm is the computation of the derivative of the structural displacement field given the derivative of the aerodynamic load $\left(d\boldsymbol{f}_{ae}{}^{(m+1)}/ds_l\right)$ computed in the fluid subproblem:

$$\mathbf{K}(\boldsymbol{u}^{(n)})\frac{d\tilde{\boldsymbol{u}}}{ds_l}^{(m+1)} - \mathbf{T}_f\left(\frac{\partial\boldsymbol{f}_\Gamma}{\partial\boldsymbol{x}}\frac{d\boldsymbol{x}}{ds_l}^{(m+1)} + \frac{\partial\boldsymbol{f}_\Gamma}{\partial\boldsymbol{w}}\frac{d\boldsymbol{w}}{ds_l}^{(m+1)}\right) = -\left(\frac{\partial\boldsymbol{f}_{int}}{\partial s_l}^{(m+1)} - \frac{\partial\boldsymbol{f}_{ext}}{\partial s_l}^{(m+1)}\right) \tag{23}$$

Similarly to the displacement computation in a NLBGS algorithm, the derivative of the structural displacement in the LBGS algorithm is under-relaxed by using a Successive Over-Relaxation technique to avoid instability problems. A

constant or an adaptive (Aitken's) relaxation factors can be applied (equation 24). The convergence and stability of the LBGS algorithm is strongly dependent on the appropriate choice of $\theta^{(m)}$, mainly because the Jacobian matrix of the GSE is ill-conditioned when evaluated at the aeroelastic steady state.

$$\frac{d\boldsymbol{u}}{ds_l}^{(m+1)} = (1-\theta^{(m)})\frac{d\boldsymbol{u}}{ds_l}^{(m)} + \theta^{(m)}\frac{d\tilde{\boldsymbol{u}}}{ds_l}^{(m)} \tag{24}$$

$$\frac{d\boldsymbol{u}}{ds_l}^{(m+1)} \rightarrow \frac{d\mathbf{x}_\Gamma}{ds_l}^{(m+1)} = \mathbf{T}_u\frac{d\boldsymbol{u}}{ds_l}^{(m+1)} \tag{25}$$

The under-relaxed derivative of the structural displacement is transferred to the fluid domain over the fluid-structure interface, thus closing the iterative loop. Finally, a check to monitor convergence is evaluated in each iteration of the LBGS algorithm.

$$\left\| \mathbf{H}\frac{d\boldsymbol{w}}{ds_l}^{(m+1)} + \frac{\partial \mathbf{F}}{\partial s_l} + \frac{\partial \mathbf{F}}{\partial \boldsymbol{x}}\frac{d\boldsymbol{x}}{ds_l}^{(m+1)} \right\|_2 \leq \epsilon_F^{SA} \left\| \mathbf{H}\frac{d\boldsymbol{w}}{ds_l}^{(0)} + \frac{\partial \mathbf{F}}{\partial s_l} + \frac{\partial \mathbf{F}}{\partial \boldsymbol{x}}\frac{d\boldsymbol{x}}{ds_l}^{(0)} \right\|_2 \tag{26}$$

where ϵ_S^{SA} is the specified tolerance for the fluid and structure subproblems in the sensitivity analysis procedure. The evaluation of the inequality related to the structure subproblem (equation 26) is sufficient for the convergence check. The fluid subproblem is automatically converged when the structure subproblem inequality is satisfied.

4.3 Schur-Krylov scheme

An alternative sensitivity analysis solution methodology is proposed, for solving the stability issues caused by the ill-conditioned operator of the GSE. The approach consists in using a Schur complement formulation to condense the GSE (equation 17) on the derivative of the degrees of freedom of the mesh on the fluid-structure interface $\left(d\boldsymbol{x}_\Gamma/ds_l\right)$.

$$\mathbf{J}_Z\frac{d\mathbf{x}_\Gamma}{ds_l} = -\frac{\partial \mathbf{x}_\Gamma}{\partial s_l} - \mathbf{T}_u\mathbf{K}^{-1}\left[\frac{\partial \boldsymbol{f}_{int}}{\partial s_l} - \frac{\partial \boldsymbol{f}_{ext}}{\partial s_l} + \mathbf{T}_f\frac{\partial \boldsymbol{f}_\Gamma}{\partial \boldsymbol{w}}\mathbf{H}^{-1}\frac{\partial \mathbf{F}}{\partial s_l}\right] \tag{27}$$

The reduced linear system of equations (27) is solved by a Krylov method. The matrix-vector product of $\mathbf{J}_Z$ with a Krylov vector $\boldsymbol{p}_\Gamma^{(k)}$ is equal to the one described on reference (Barcelos, Bavestrello and Maute, 2006). A summary of well known numerical methods and preconditioning techniques for solving large symmetric and unsymmetric linear system of equations are described on reference (Saad, 2003).

5. Numerical Results

The verification of the analytical sensitivities is the most important step before applying them to a design optimization process. The analytical sensitivities are verified against numerical sensitivities obtained by finite difference. The aeroelastic problem selected for the verification is an long span wing used for a study of different analytical sensitivity analysis setups. In the sequence, a problem evaluates the performance of the design optimization of a realistic wing. This problem represents the final step on the verification of the analytical sensitivities.

The problems are solved by a finite volume Euler/Navier-Stokes code featured with moving grids and coupled to a finite element structural code. The linearized fluid subproblem is solved by a parallel GMRES method equipped with full matrix and matrix-free matrix-vector product techniques which is preconditioned by the Restricted Additive Schwarz (RAS) method. The linearized mesh-motion subproblem is solved with a parallel preconditioned Conjugated Gradient (PCG) method. To guarantee a smooth convergence rate, the aeroelastic analysis employs a NLBGS algorithm with a weak coupling between the averaged Navier-Stokes equations and the Spalart-Allmaras turbulence model equation. The global sensitivity equations (GSE) are solved by LBGS and SK algorithms. The accuracy of the solution of the fluid sub-problem is guaranteed by the use of a second order reconstruction of the fluid variables over the grid cells.

For the aeroelastic problems the structure is treated as linear. Every test case has structured mesh layers disposed close to the wall to approximate the flow in the boundary layer. The law of the wall is employed to complement the viscosity computation in the boundary layer. The law of the wall employed in this work is the Reichardt's law (Kestin and Richardson, 1963, Autret Grandotto and Dekeyser, 1987). The structured mesh layers are disposed in a way that the inner and outer regions of the boundary layer are fully covered. The number of layers is also chosen to match the mesh refinement of the wall, avoiding the generation of extremely stretched mesh elements which could lead to an increase in "stiffness" of the fluid subproblem (Soto, Lohner and Camelli, 2002). The computation of test cases was carried out on different set of computers: an Intel Xeon cluster with 128 processors and 1GB RAM per processor; an AMD Opteron cluster with 128 processor and 2GB RAM per processor.

5.1 Verification of viscous turbulent analytical sensitivities using a long span wing

The conclusive test for the verification of the analytical sensitivities is done with an aerodynamic profile under general flow conditions. For this purpose, a turbulent flow over a long span wing with a NACA 0012 airfoil section is selected. A wing with a NACA 0012 airfoil section was chosen as a test case because a large experimental flow data base is available for this specific geometry (Guezaine, 1999). In addition, a simple geometry allows for the creation of meshes with relative small amount of degrees of freedom. This reduces the computational cost, and consequently allows for the execution of more test runs. Other than that, the flow over the long span wing has a stable quasi-2D profile, and yet tridimensional flow structures and effects such as vorticity and turbulence are captured.

Table 1. Material properties and free-stream configuration for the long sapn wing.

Material Properties	
Young's modulus E	$7.31 \times 10^{10}\ N/m^2$
Poisson ratio ν	0.33
Thickness	$0.02\ m$
Density ρ	$2,700\ kg/m^3$
Linear spring stiffness K_L	$1,000\ N/m^2$
Torsional spring stiffness K_Θ	$75\ N$
Fluid Parameters	
Angle of attack α	1.77^o
Yaw angle β	0^o
Mach number M_∞	0.502
Density ρ_∞	$1.4643\ kg/m^3$
Pressure p_∞	$125,341\ N/m^2$
Reynolds number Re	2.91×10^6

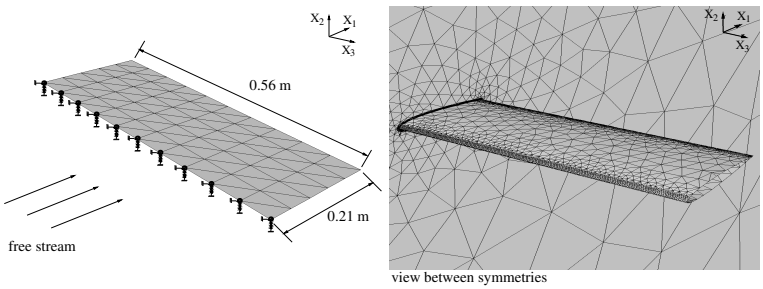

Figure 1. Mesh discretization of the long span wing.

The airfoil section has 0.21m of chord and a wing span of 0.56m. The fluid mesh has a total of $55,363$ grid points, which leads to $332,172$ fluid state variables and $166,089$ mesh-motion degrees of freedom (figure 1). A total of 10 layers of structured mesh elements with a linear growth ratio of 1.8 and an initial gap of $1.2 \times 10^{-4}\ m$ is set in the boundary layer. Usually, the boundary layer variables are specified in a way to balance the correct representation of the flow at that region, and the mesh quality of the mesh over the mesh motion process. The viscosity computation in the boundary layer is complemented using the law of the wall with a distance to the wall of $1.0 \times 10^{-4}\ m$. The skin of the airfoil has no structural function. Thus, a plate with dimension equal to the middle plane of the airfoil is used as the structure and is composed of 100 3-nodes shell elements (figure 1). The aeroelastic effects on the airfoil structure, other than the flexibility of the plate, are emulated by the inclusion of linear and torsional spring elements at the leading edge of the airfoil, attached to the plate extremity. More details about the material properties and the flow configuration are shown in table 1.

The sensitivity analysis for the long span wing consists of the computation of the derivative of the drag force (D), the lift force (L) and the aerodynamic moment (M) with respect to the design variables: vertical motion of the plate trailing edge (s_1), plate thickness (s_2), Mach number (s_3) and angle of attack (s_4). The aerodynamic moment is computed in relation to the point ($x_1 = 6.095\ m$, $x_2 = -0.100\ m$, $x_3 = 0.280\ m$) located on the perpendicular intersection of the fluid domain middle plane and the axis where the spring elements are attached. The leading edge of the long span wing is located on the straight line defined by points ($x_1 = 6.190\ m$, $x_2 = 0.000\ m$, $x_3 = 0.000\ m$) and ($x_1 = 6.190\ m$, $x_2 = 0.000\ m$, $x_3 = 0.560\ m$). The numerical sensitivities are computed by a central finite difference scheme and the

fluid subproblem in the analytical sensitivity analysis is solved with the exact linear operator to guarantee the best solution accuracy. This test accounts for a variety of design variables, other than shape, making it an excellent choice to develop a sensitivity verification study. One of the reasons for this test lies in the different possibilities of design variables, besides than shape that can be employed. To guarantee the accuracy of the numerical and the analytical sensitivities, convergence tolerances of $\epsilon = 10^{-5}$ are applied to the aeroelastic and sensitivity analyses. As a result, the sensitivity analysis computation is based on well defined aeroelastic states: D=82.8N, L=224.50N and M=1129.47Nm.

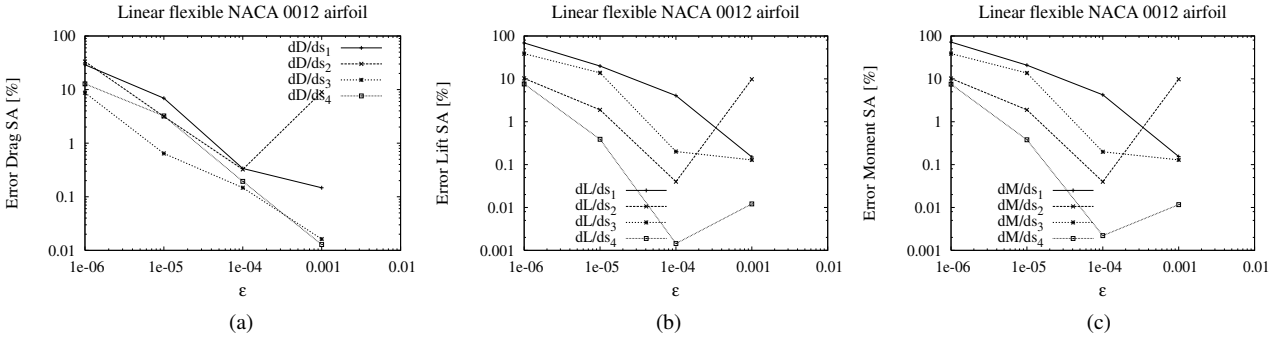

Figure 2. Error of the sensitivities of drag and lift of the turbulent flow over the long span wing using a LBGS solver.

Table 2. Analytical sensitivities of the turbulent flow over the long span wing.

Structure	$\frac{dD}{ds_1}\ [N/m]$	$\frac{dD}{ds_2}\ [N/m]$	$\frac{dD}{ds_3}\ [N]$	$\frac{dD}{ds_4}\ [N]$
LBGS	-29.1289058	51.9767741	286.650701	93.6341001
SK	-29.1288062	51.9771019	286.650995	93.6345905
Structure	$\frac{dL}{ds_1}\ [N/m]$	$\frac{dL}{ds_2}\ [N/m]$	$\frac{dL}{ds_3}\ [N]$	$\frac{dL}{ds_4}\ [N]$
LBGS	-3,009.12525	7,399.21587	355.091866	7,392.02043
SK	-3,009.12076	7,399.21681	355.090665	7,392.02634
Structure	$\frac{dM}{ds_1}\ [N]$	$\frac{dM}{ds_2}\ [N]$	$\frac{dM}{ds_3}\ [Nm]$	$\frac{dM}{ds_4}\ [Nm]$
LBGS	-1,439.77592	37,004.8396	1,803.58725	37,214.8868
SK	-1,439.77363	37,004.8457	1,803.58134	37,214.9152

The reference analytical gradients for the linear flexible structure are shown in table 2. The analysis of figure 2 shows that the difference for the best numerical and analytical sensitivity comparison is no greater than 0.5%. Considering the turbulent flow configuration employed, this error represents an excellent agreement among analytical and numerical sensitivities. Results for the sensitivities obtained with the SK solver are shown in table 2. The data show that a difference of 0.001% with respect to the reference sensitivities computed with the LBGS solver is observed. The SK solver provides an alternative to the sensitivity computation. The SK solver has also shown a significant reduction in sensitivity analysis computational time.

5.2 Design optimization of a realistic wing under transonic turbulent flight conditions

A complete design optimization of a realistic aeroelastic system is setup to finally verify the viscous turbulent sensitivity analysis. The test case is NASA's Aeroelastic Research Wing (ARW2) (Farhangnia, Guruswamy and Biringen, 1996), which was also used for performance verification of the SK method. The finite element model of the ARW2 structure contains 11,838 degrees of freedom. The fluid domain is represented by a tridimensional unstructured mesh with 149,826 grid points, which leads to a total of 898,956 fluid-state variables and 449,478 degrees of freedom for the mesh motion subproblem. The boundary layer is populated with 15 layers of structured mesh elements with a linear growth ratio of 1.2 and an initial gap of $3.048 \times 10^{-4}\ m$. The law of the wall is employed, and the distance to the wall is $2.540 \times 10^{-4}\ m$. All input data relevant to the aeroelastic analysis are shown in table 3.

The objective of the design optimization problem is to minimize the drag. The optimization procedure is subjected to criteria such as: drag force, lift force, displacements of the tip of the wing, and von Mises stresses on stiffeners. The design variables are associated with the shape of the wing: s_1 and s_2 are respectively the backsweep and the twisting of the wing, and s_3, s_4 and s_5 represent the thickness of the stiffeners. The design optimization problem has constraints on the lift value, the von Mises stress of the stiffeners and the vertical displacement of points C and D located at the wing tip, figure

Table 3. Material properties, geometry dimensions and flight configuration for the ARW2.

Material Properties and Geometry	
Young's modulus E	$7.1 \times 10^{10}\ N/m^2$
Poisson ratio ν	0.32
Density ρ	$2,794\ kg/m^3$
Fluid Properties	
Altitude H	$12,200\ m$
Angle of attack α	2.5^o
Yaw angle β	0^o
Mach number M_∞	0.8
Density ρ_∞	$0.2928\ kg/m^3$
Pressure p_∞	$18,828\ N/m^2$
Reynolds number Re	4.94×10^6

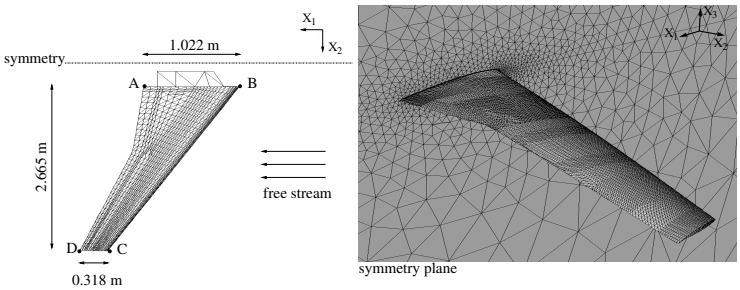

Figure 3. Design model of the ARW2.

3. The stress and the vertical displacement can not exceed: $\sigma_{max} = 1.13 \times 10^8 N/m^2$ and $u_{max} = 0.381m$. The mesh motion solver employs a linear finite element formulation that simplifies the construction of the mesh pseudo stiffness matrix to reduce the computational time, instead of the traditional torsional spring method. In addition, the sensitivity analysis accuracy is reinforced by using the exact linear operator for solving the fluid subproblem. The tolerance value of about 10^{-5} is applied to the aeroelastic and sensitivity analyses. For comparison, the optimization is divided in different tests, one for the LBGS solver with a fixed relaxation strategy ($\theta = 0.5$), and the other for the SK solver with a fixed relaxation strategy ($\theta = 1.0$).

For both tests, the minimization of D leads to almost the same results (table 4): about 27% reduction. In the current optimization setup every design variable is related to the wing shape. The comparison of the final optimization results by using the LBGS and SK solvers shows that their performance in time are almost identical, 4. The results in figures 4a and 4b shows that the test **SK** has the best performance. The LBGS method spends more time, and this behavior is expected, indicating the superior performance of the SK method over the LBGS method for solving the sensitivity analysis in a optimization framework.

Table 4. Aeroelastic performance and design variables at the optimum.

	$D\ [N]$	$L\ [N]$	D/L	$u_C\ [m]$	$\sigma_{max}\ [N/m^2]$
LBGS	715.46	5644.39	0.1268	0.1421	5.60 10^7
SK	715.62	5644.39	0.1268	0.1421	5.60 10^7
	$s_1\ [m]$	$s_2\ [m]$	$s_3\ [m]$	$s_4\ [m]$	$s_5\ [m]$
s_l^L	-0.635000	-0.025400	-0.002565	-0.000762	-0.000762
s_l^U	0.635000	0.010160	0.012700	0.038100	0.038100
LBGS	0.635000	-0.007028	-0.002565	-0.000762	-0.000762
SK	0.635000	-0.007031	-0.002565	-0.000762	-0.000762

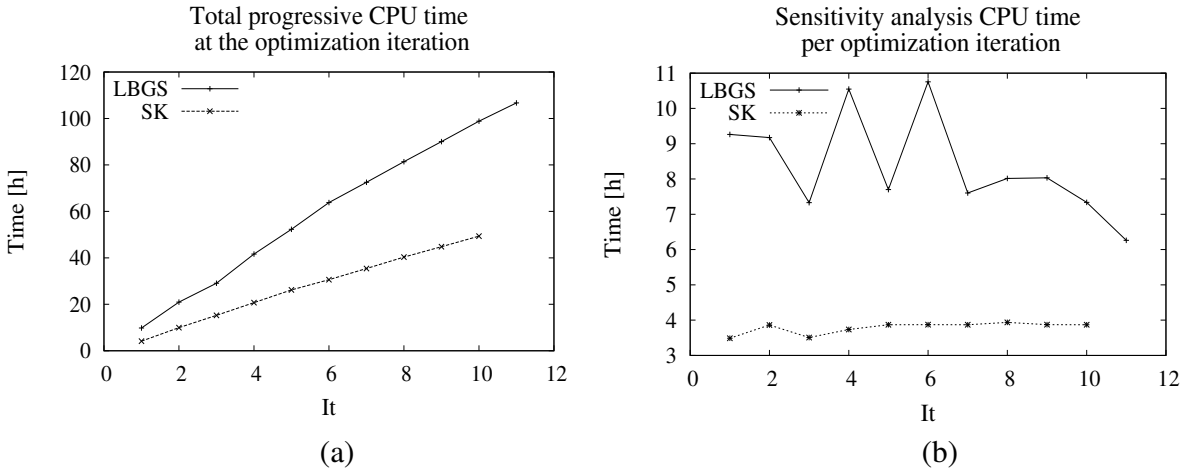

Figure 4. CPU time history: (a) Total progressive time history, (b) Time spent per sensitivity analysis.

6. Conclusions

The main goal of this work was to develop a computationally robust and efficient sensitivity analysis methodology for the design optimization of realistic aeroelastic systems. This work was motivated by the growing demand for high-fidelity design optimizations of large-scale aeroelastic systems. To achieve this goal, methodologies employed in previous works for inviscid aeroelastic problems (Maute, Nikbay and Farhat, 2001a, Nikbay, 2002) were extended to viscous and turbulent aeroelastic problems. An analytical sensitivity analysis was developed based on different discretizations of the flow equations such as the Euler equations, the instantaneous Navier-Stokes equations, and the averaged Navier-Stokes equations closed with the Spalart-Allmaras turbulence model. The most important achievement in this work was the verification of the analytical sensitivity analysis for viscous turbulent flows over different aeroelastic geometries. The analytical sensitivities computed using the LBGS and SK methods were verified against finite difference sensitivities obtained for a large range of perturbations. The conclusive verification of the analytical sensitivities was accomplished by using an long span NACA0012 wing under realistic flow conditions. A difference of no more than 0.5% between analytical and numerical sensitivities was obtained. This is also an excellent result, and is due in part to the slim airfoil geometry. The final step in this work was the application of the viscous turbulent analytical sensitivity analysis in the optimization of a realistic aeroelastic system. For this purpose, a well known aeroelastic test case was chosen, the ARW2. The main conclusion is that SK method to the design sensitivity analysis improves both the robustness and efficiency when compared to the traditional LBGS method.These results reaffirm the superiority of the SK method over the LBGS method.

7. REFERENCES

Barthelemy, J.-F., Wrenn, G., Dovi, A. and Hall, L., 1994, "Supersonic transport wing minimum design integrating aerodynamics and structures", Journal of Aircraft, Vol. 31, No. 2, pp. 330-338.

Turgeon, É., Pelletier, D. and Borggaard, J., 2004, "A general continuous sensitivity equation formulation for the ϵ - κ model of turbulence", International Journal of Computational Fluid Dynamics, Vol. 18, No. 1, pp.29-46.

Pajot, J. M. and Maute, K., 2006, "Analytical sensitivity analysis of geometrically nonlinear structures based on the co-rotational finite element method", Finite Elements in Analysis and Design, Vol. 42, No. 10, pp. 900-913.

Guezaine, P., 1999, "An implicit upwind finite volume method for compressible turbulent flows on unstructured meshes", PhD thesis, Faculté des Sciences Appliquées, Université de Liège.

Cebeci, T., 2004, "Analysis of turbulent flows", Elsevier.

Degand, C. and Farhat, C., 2002, "A three-dimensional torsional spring analogy method for unstructured dynamic meshes", Computers and Structures, Vol. 80, pp. 305-316.

Nikbay, M., 2002, "Coupled sensitivity analysis by discrete-analytical direct and adjoint methods with applications to aeroelastic optimization and sonic boom minimization", PhD thesis, Department of Aerospace Engineering, University of Colorado.

Lund, E. and Møller, H. and Jakobsen, L.A., 2003, "Shape design optimization of stationary fluid-structure interaction problems with large displacements and turbulence", Structural and Multidisciplinary Optimization, Vol. 25, No. 5-6, pp. 383-392.

Farhat, C., Geuzaine, P. and Brown, G., 2003, "Application of a three-field nonlinear fluid-structure formulation to the

prediction of the aeroelastic parameters of an F-16 fighter", Computers and Fluids, Vol. 32, pp. 3-29.

Maute, K., Nikbay, M. and Farhat, C., 2001, "Coupled analytical sensitivity analysis and optimization of three-dimensional nonlinear aeroelastic systems". AIAA Journal, Vol. 11, No. 11, pp. 2051-2061.

Barcelos, M., Bavestrello, H. and Maute, K., 2004, "Efficient solution strategies for steady-state aeroelastic analysis and design sensitivity analysis", In 10th AIAA/ISSMO multidisciplinary optimization conference, August 30 - September 1, Albany, NY.

Barcelos, M., Bavestrello, H. and Maute, K., 2006, "A schur-newton-krylov solver for steady-state aeroelastic analysis and design sensitivity analysis", Computer Methods in Applied Mechanics and Engineering, Vol. 195, No. 17-18, pp. 2050-2069.

Farhat, C., Lesoinne, C. and LeTallec, P., 1998, "Load and motion transfer algorithms for fluid/structure interaction problems with non-matching discrete interfaces: momentum and energy conservation, optimal discretization and application to aeroelasticity", Computer Methods in Applied Mechanics and Engineering, Vol. 157, pp. 95-114.

Batina, J. T., 1991, "Unsteady Euler algorithm with unstructured dynamic mesh for complex-aircraft aerodynamic analysis", AIAA Journal, Vol. 29, No. 3, pp. 327-333.

Sobieszczanski-Sobieski, J., 1990, "Sensitivity of complex, internally coupled systems", AIAA Journal, Vol. 28, No. 1, pp. 153-160.

Vrahatis, M. N., Magoulas, G. D. and Plagianakos, V. P., 2003, "From linear to nonlinear iterative methods", Applied Numerical Mathematics, Vol. 45, pp. 59-77.

Farhat, C. and Lesoinne, M., 2000, "Two efficient staggered algorithms for the serial and parallel solution of three-dimensional nonlinear transient aeroelastic problems", Computer Methods in Applied Mechanics and Engineering, Vol. 182, pp. 499-515.

Maute, K., Nikbay, M. and Farhat, C., 2001, "Sensitivity analysis and design optimization of three-dimensional nonlinear aeroelastic systems by the adjoint method", International Journal for Numerical Methods in Engineering, Vol. 56, No. 6, pp. 911-933.

Saad, Y., 2003, "Iterative methods for sparse linear systems", SIAM.

Kestin, J. and Richardson, P. D., 1963, "Heat transfer across turbulent, incompressible boundary layers", International Journal of Heat and Mass Transfer, Vol. 6, pp. 147-189.

Autret, A., Grandotto, M. and Dekeyser, I., 1987, "Finite element computation of a turbulent flow over a two-dimensional backward facing step", International Journal for Numerical Methods in Fluid, Vol. 7, No. 2, pp. 89-102.

Soto, O., Lohner, R. and Camelli, F., 2002, "A linelet preconditioner for incompressible flow solvers", International Journal of Numerical Methods for Heat & Fluid Flow, Vol. 13, No. 1, pp. 133-147.

Farhangnia, M., Guruswamy, G. and Biringen, S., 1996, "Transonic-buffet associated aeroelasticity of a supercritical wing", In AIAA 1996-0286, 34th Aerospace Sciences Meeting & Exhibit, Jan 15-18, Reno, NV.